

New Insights on the Behavior of PRODAN in Homogeneous Media and in Large Unilamellar Vesicles

Fernando Moyano, M. Alicia Biasutti, Juana J. Silber,* and N. Mariano Correa*

Departamento de Química, Universidad Nacional de Río Cuarto, Agencia Postal # 3, X5804ZAB Río Cuarto, Argentina

Received: December 9, 2005; In Final Form: March 30, 2006

The behavior of 6-propionyl-2-dimethylaminonaphthalene (PRODAN) was studied in homogeneous media and in large unilamellar vesicles (LUVs) of the phospholipid 1,2-di-oleoyl-*sn*-glycero-3-phosphatidylcholine (DOPC), using absorption, emission, depolarization, and time-resolved spectroscopies. In homogeneous media, the Kamlet and Taft solvatochromic comparison method quantified solute–solvent interactions from the absorption and emission PRODAN bands. These studies demonstrate that the absorption band is sensitive to the polarity–polarizability (π^*) and the hydrogen bond donor ability (α) parameters of the media. PRODAN in the excited state is even more sensitive to these parameters and to the hydrogen bond acceptor ability (β) of the media. The transition energy (expressed in kcal/mol) for both absorption and emission bands gives a linear correlation with the well-known polarity parameter $E_{T(30)}$. The results from the absorption and emission bands also reveal that PRODAN aggregates in water. The monomer has two fluorescence lifetimes, 2.27 and 0.65 ns, while the aggregate has a lifetime of 14.6 ns. Using steady-state anisotropy measurements, the calculated volumes of the aggregate and the monomer are 5590 and 222 mL mol^{−1}, respectively. In DOPC LUVs, PRODAN undergoes a partition process between the water bulk and the DOPC bilayer. We show that the partition constant (K_p) value is large enough that only at [DOPC] below 0.15 mg/mL PRODAN in water can be detected. PRODAN dissolved in LUVs at [DOPC] > 1 mg/mL exists completely incorporated in its monomer form and senses two different microenvironments within the bilayer: a polar region in the interface near the water and a less polar and also less viscous environment, between the phospholipid tails. These environments were characterized by their fluorescence lifetimes (τ), showing that PRODAN in the polar microenvironment has a τ value of approximately 4 ns while in the less polar region gives a value of 1.2 ns. Moreover, this probe also senses the micropolarity of these two different regions of the bilayer and yields values similar to that of methanol and tetrahydrofuran.

Introduction

Organized molecular assemblies, such as vesicles or liposomes, can be considered as large cooperative units with very different characteristics from the individual structural units which constitute them.¹ Phospholipids are the fundamental matrix of natural membranes and represent the environment in which many proteins and enzymes display their activity.² The problems associated with the wide diversity in composition and structure of biological membranes are avoided if one uses synthetic liposomes or vesicles which mimic the geometry, topology, and skeletal structure of cell membranes but lack ion channels and the multitude of other embedded components such as proteins.^{3–7} Results using small unilamellar vesicles (SUVs) as model systems for cells are often controversial because of their size and bilayer defects due to the high curvature. For this reason, it is common to use large unilamellar vesicles (LUVs) to get closer to cell-like structures.⁸

On the other hand, interactions of small molecules with membranes are important issues in membrane biology. Understanding their role in modulating the structure and function of biological membranes requires knowledge of the location of the molecules and the degree of perturbation that it may cause in

them. Many aspects of this subject were investigated in model membrane systems using different spectroscopic techniques in order to characterize the membrane structure and dynamics.^{9–11} Fluorescence spectroscopy has several advantages including a high sensitivity, a noninvasive nature, an intrinsic time scale, and an excellent response to the physical properties of the membrane.^{1,12,13} In general, for a fluorophore in a bulk no viscous solvent, the dipolar relaxation of the solvent molecules around its excited state is much faster than the fluorescence lifetime. In this way, the wavelength of maximum emission usually is independent of the excitation wavelength when only one species and an $S_0 \rightarrow S_1$ transition are involved. However, excitation wavelength dependence is observed if the dipolar relaxation of the solvent molecules is slow in the excited state, such that the relaxation time is comparable to or longer than the fluorescence lifetime. Such a shift in the wavelength of maximum emission toward higher wavelengths, caused by a shift in the excitation wavelength toward the red edge of the absorption band, is known as the red-edge excitation shift (REES). This effect is mostly observed with polar fluorophores, whose motion is restricted by media such as very viscous solutions or condensed phases.^{1,14–17} Accordingly, the REES can serve as an indicator of the fluorophore microenvironment.

It is well-known that 6-propionyl-2-dimethylaminonaphthalene (PRODAN) is a probe particularly sensitive to the polarity

* To whom correspondence should be addressed. E-mail: jsilber@exa.unrc.edu.ar (J.J.S.); mcorrea@exa.unrc.edu.ar (N.M.C.).

and hydrogen bond capacity of the microenvironment.^{18–23} It is a fluorescent probe that exhibits strong shifts in the absorption and emission spectra with solvent characteristics,^{18,20–22} and it has been extensively employed in phospholipid model systems to investigate the nature of lipid domains, phase coexistence, and phase interconversion.^{19,24–27} It has also been used to monitor relevant differences in the polarity of the different phase states^{24,25,28,29} and the influence of cholesterol¹⁹ and alcohol molecules.^{28,29} Moreover, the effects of the hydrostatic pressure on the location of PRODAN in lipid bilayers have been studied using emission³⁰ and FT-IR⁹ spectroscopy. The results show that the probe favors a more hydrophobic environment under pressure. However, Krasnowska et al.²⁴ suggested that the proposed attribution of PRODAN emission features to the probe location at various depths along the bilayers is unlikely because the probe partition between the bilayer and water depends on the phospholipid phase states and on the membrane fluidity. Indeed, the PRODAN partition coefficient is higher in the liquid-crystalline phase with respect to the gel for a factor of about 30.

It is generally assumed that the probe reports primarily on the internal solvent environment through changes in emission wavelength, lifetime, or anisotropy, but there is some controversy in the subject.^{31–33} An interesting feature that has been described for this probe is a concentration-dependent aggregation phenomenon in water, producing an emission band with a peak at 430 nm³¹ which is not the consequence of impurities in the commercial PRODAN preparation, as was previously suggested.³³ On the other hand, to the best of our knowledge, there are no reports in the literature dealing with the possibility of the PRODAN aggregation process in the phospholipid bilayer.

In light of these facts, the aim of this contribution is to try to clarify the aggregation process of PRODAN in water studying the aggregate using absorption, emission, and steady-state and time-resolved fluorescence spectroscopies. Furthermore, here, we extend the study to the behavior of PRODAN in LUVs of 1,2-di-oleoyl-*sn*-glycero-3-phosphatidylcholine (DOPC) to investigate the micropolarity and the microviscosity of the bilayer. The results clearly reveal that PRODAN aggregates in water but not when it is in the LUV bilayer. In addition, once the molecular probe is totally incorporated into the bilayer, the probe does not partition to the water and exists in two different environments with different micropolarities and microviscosities.

Experimental Section

The lipid 1,2-di-oleoyl-*sn*-glycero-3-phosphatidylcholine (DOPC, $T_c = -17.3$ °C^{6,34}) in chloroform, as obtained from Avanti Polar Lipids, Inc. (Alabaster, AL), and the fluorescent probe 6-propionyl-2-dimethylaminonaphthalene (PRODAN), from Molecular Probes (Eugene, OR), have been used without further purification. At the temperature used in the experiments (25 ± 0.1 °C), the DOPC LUV system is composed of a pure liquid-crystalline phase.³⁴

To perform the study in pure solvent, an appropriate amount of PRODAN stock solution in acetonitrile (Sintorgan, HPLC grade) was transferred into the volumetric flask using a calibrated microsyringe. The solvent was evaporated by bubbling dry N₂ and the residue dissolved in the appropriate solvent (Sintorgan, HPLC grade) to obtain a final PRODAN concentration of 5×10^{-6} M. The solvent set was chosen to cover a range as wide as possible in the various solvent characteristics.

The vesicle solutions loaded with PRODAN were typically prepared as follows: the stock lipid solution was prepared by mixing the appropriate amount of DOPC and PRODAN in chloroform (Sintorgan, HPLC grade). After the solvent was evaporated and the film was dried under reduced pressure, large multilamellar vesicles (MLVs) were obtained by hydrating the dry lipid-dye film with water through mixing (Vortex, 2-Genie) for about 5 min at room temperature. The resulting solution of MLVs has the desired lipid and PRODAN concentration. To prepare large unilamellar vesicles (LUVs), the MLV suspension was extruded 10 times (Extruder, Lipex biomembranes) through two stacked polycarbonate filters with a pore size of 200 nm under a nitrogen pressure of up to 3.4 atm. The unilamellar nature of pure DOPC vesicles prepared using the extrusion method³⁵ had been confirmed previously^{4,5,7,36} by measuring the extent of quenching by Mn²⁺ of their ³¹P NMR signals.³⁷ To subtract the background contribution of the absorption and emission, samples of the same phospholipids and at the same concentrations were prepared, omitting the addition of the probe. All samples were used immediately after preparation.

Ultrapure water was obtained from Labonco equipment model 90901-01.

The absorption spectra were measured by using a Shimadzu 2401 instrument at 25 ± 0.1 °C unless otherwise indicated. A Spex fluoromax apparatus was employed for the fluorescent measurements. Corrected fluorescence spectra were obtained using the correction file provided by the manufacturer. The path length used in the absorption and emission experiments was 1 cm. λ_{max} was measured by taking the midpoint between the two positions of the spectrum where the absorbance is equal to $0.9A_{\text{max}}$. The uncertainties in λ_{max} are about 0.1 nm.

Stationary anisotropy measurements were performed with a Hitachi 2500 spectrofluorometer with a Glam-Thomson polarizer for the excitation and analyzer polarizer. In vesicles (LUVs) of DOPC, background fluorescence, as well as light scattering, was removed by subtraction of a spectrum recorded on a blank solution. Fluorescence anisotropy $\langle r \rangle$ values were obtained at 25 °C using the expression $\langle r \rangle = (I_{\text{VV}} - GI_{\text{VH}})/(I_{\text{VV}} + 2GI_{\text{VH}})$, where I_{VV} and I_{VH} are the vertically and horizontally polarized components of PRODAN after excitation by vertically polarized light and G is the sensitivity factor of the detection system.¹⁴

Steady-state anisotropy measurements were converted to rotation correlation time (ϕ) using the following equation:

$$r = \frac{r_0}{1 + (\tau/\phi)} \quad (1)$$

where r is the measured fluorescence anisotropy, r_0 is the fundamental anisotropy, and τ is the corresponding fluorescence lifetime. A fundamental anisotropy of 0.336 was used for PRODAN.³⁸

The rotational correlation times (ϕ) were used to determine the volume of the rotating unit (V) (mL mol⁻¹) for monomer and aggregate forms of the probe in solution using the Perrin equation:

$$\phi = \frac{\eta V}{RT} \quad (2)$$

where η is the viscosity (0.0010 kg m⁻¹ for water at 293 K), R is the gas constant (8.314 kg m⁻² s⁻² K⁻¹ mol⁻¹), and T is the temperature in kelvins.³²

To apply the Kamlet–Taft solvatochromic comparison method (KTSCM) to the emission frequency and considering that the maximum frequency of an emission spectrum is not necessarily

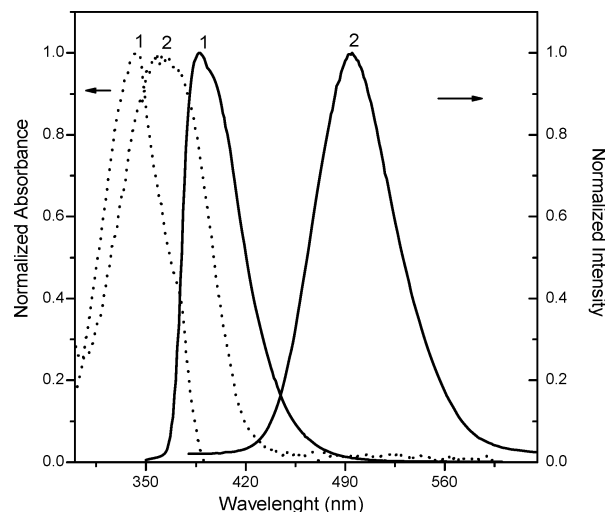


Figure 1. Normalized absorption (···) and emission (—) spectra of PRODAN in homogeneous media: (1) *n*-heptane; (2) methanol. [PRODAN] = 5×10^{-6} M.

the maximum of the spectrum on a wavelength scale, a correction was performed.¹⁴ Thus, the emission spectrum on a wavelength scale was multiplied by the square of the wavelength and replotted (as $F(\nu) = (\lambda^2) F(\lambda)$ vs frequency (ν)) to find the maximum.

Fluorescence decay data were measured with the time correlated single photon counting technique on Edinburgh Instrument FL-9000 equipment. Fluctuations in the pulse and intensity were corrected by making an alternate collection of scattering and sample emission. The quality of the fits was determined by the reduced χ^2 value.³⁹

Results and Discussion

Study in Homogeneous Media. To gain more insight about the behavior of the molecular probe PRODAN in LUVs of DOPC, we first characterized the photophysical properties of the dye in homogeneous media. Figure 1 shows typical normalized absorption and emission spectra of PRODAN in a nonpolar environment like *n*-heptane and in a polar and hydrogen bond donor environment like methanol. The probe shows a bathochromic shift in both absorption and emission bands upon changing the solvent properties.

There have been different approaches to understanding the solvatochromic behavior of PRODAN using absorption and emission spectroscopy of the molecular probe in different polar and nonpolar solvents.^{18–22} The studies were extended to a series of alkanols, and it was demonstrated, in a qualitative way, that the probe is extremely sensitive to both the polarity and hydrogen bond donor abilities of the solvent.^{20,29} On the other hand, Catalan et al.^{21,23} quantified the specific interactions between PRODAN and different pure and mixed solvents and showed that the emission band of the probe is sensitive to the parameters SA (solvent acidity), SB (solvent basicity), and SPP (solvent polarity/polarizability).²³ The absorption band of PRODAN was correlated using the Lippert equation and including the term SA that shows that the carbonyl and the amine groups are hydrogen bond donor acceptors.²³

The solvent effects on physical or chemical processes are frequently studied by empirical solvent parameters to determine the predominant interactions. One of the most useful approaches for elucidating and quantifying different solute–solvent interactions is the Kamlet–Taft solvatochromic comparison method (KTSCM).⁴⁰ In the present contribution, the different PRODAN–

TABLE 1: Wavenumbers of Absorption and Emission Maxima (10^3 cm^{-1}) for PRODAN in Different Solvents ([PRODAN] = 5×10^{-6} M)

solvent	ν_{abs}	ν_{em}	π^* ^a	α^a	β^a
<i>n</i> -hexane	29.18	25.63	−0.11	0.00	0.00
<i>n</i> -heptane	29.09	25.65	−0.08	0.00	0.00
cyclohexane	29.19	25.65	0.00	0.00	0.00
decane	29.21	25.60	0.03	0	0.00
carbon tetrachloride	28.72		0.21 ^b	0.00	0.10
diethyl ether	28.95		0.24 ^b	0.00	0.60 ^b
<i>n</i> -octanol	27.53	21.19	0.40	0.77	0.81
ethyl acetate	28.60	22.84	0.45	0.00	0.45
<i>m</i> -xylene	28.60	24.15	0.47	0.00	0.12
<i>n</i> -butanol	27.38	20.73	0.47	0.84	0.84
2-propanol	27.68	21.07	0.48	0.76	0.84
toluene	28.35	24.04	0.49 ^b	0.00	0.11 ^b
ethanol	27.59	20.35	0.54	0.86	0.75
tetrahydrofuran	28.62	23.30	0.55 ^b	0.00	0.59 ^b
benzene	28.39	23.99	0.55 ^b	0.00	0.10
methanol	27.52	19.92	0.6	0.98	0.66
acetone	28.49	22.52	0.62	0.08	0.43
glycerol	26.64	19.63	0.62	1.21	0.51
acetonitrile	28.42	21.90	0.66 ^b	0.19	0.30 ^b
chloroform	27.71		0.69 ^b	0.2	0.10
dichloromethane	28.08		0.73 ^b	0.13	0.10
<i>N,N</i> -dimethylacetamide	28.03	22.07	0.85 ^b	0.00	0.76
<i>N,N</i> -dimethylformamide	27.67	22.09	0.88 ^b	0.00	0.69
1,2-propanediol	27.18	20.02	0.92	0.9	0.52
ethylene glycol	26.80	19.76	0.92	0.9	0.52
formamide	26.90	20.10	0.97	0.71	0.48
water	27.93	19.03	1.09	1.17	0.47

^a Solvent parameters obtained from ref 41. ^b Refs 42, 43.

solvent interactions, including solvents that were not tested before for this dye, are investigated using the KTSCM method.

According to the KTSCM, absorption and emission band frequencies (ν), taken from the absorption and emission spectra of the probe, can be correlated using eq 3

$$\nu = \nu_0 + s\pi^* + a\alpha + b\beta \quad (3)$$

where π^* is the polarity/polarizability parameter, α is the hydrogen bond donor ability of the solvent, and β is the hydrogen bond acceptor or electron pair donor ability to form a coordinated bond. The s , a , and b coefficients measure the relative sensitivity of ν to the indicated solvent property.⁴¹

The absorption and emission maxima as well as the solvent parameters π^* , α , and β used for the correlation^{41–43} are given in Table 1. The PRODAN absorption and emission spectra were used to obtain the KTSCM coefficients s , a , and b which are given in eqs 4 and 5 for the absorption ($\nu_{\text{obsd}}^{\text{abs}}$) and emission ($\nu_{\text{obsd}}^{\text{em}}$) bands, respectively. The confidence level of the regression is 99.5% according to a *t*-test, n is the number of solvents used in the correlation, and r is the regression coefficient.

$$\nu_{\text{obsd}}^{\text{abs}} = 29.13 \pm 0.09 - (1.27 \pm 0.14)\pi^* - (1.18 \pm 0.10)\alpha \quad (4)$$

$$n = 26, r = 0.970$$

$$\nu_{\text{obsd}}^{\text{em}} = 25.2 \pm 0.2 - (2.6 \pm 0.2)\pi^* - (2.5 \pm 0.2)\alpha - (1.0 \pm 0.1)\beta \quad (5)$$

$$n = 23, r = 0.992$$

In the correlation of the absorption frequency (ν^{abs}) (eq 4), water has been excluded and the reason for this will be given in detail below.

The results obtained from the absorption bands (eq 4) reflect the interactions of the dye in its ground state. Here, the molecule displays a bathochromic shift with π^* and α parameters. The s/a ratio of ~ 1.1 demonstrates a slightly higher sensitivity to the polarity (π^*) than to the hydrogen bond donor capability (α) of the media. The sensitivity of PRODAN to the α parameter is expected, as it can accept a hydrogen bonding interaction through its carbonyl group as was previously suggested.^{21,23} The fact that water does not fit in the correlation indicates that another phenomenon not included in eq 4 occurs. For example, an aggregation process that PRODAN can undergo as shown in the next section.

On the other hand, the results from emission showed in eq 5 show that the excited state of PRODAN experiences a bathochromic shift with the π^* , α , and β parameters. Also, the excited state of the dye is almost twice as sensitive to the π^* and α parameters than it is in its ground state. These results confirm what was previously suggested,²⁰ that the very large Stokes shifts of PRODAN are due to the hydrogen bonding interaction between this molecule and the environment which is enhanced following the transition to the more polar excited state. The large increase in the polarity of the molecule, due to the increase of its dipole moment upon its excitation,²⁰ is the responsible of the larger sensitivity to the π^* parameter and the correlation with the electron donor ability of the solvent (β) found for the excited state.

On the other hand, it is noteworthy that the transition energy (expressed in kcal mol⁻¹) of the PRODAN absorption and emission maxima frequency can be used as a polarity parameter, E_{PRODAN} , similar to Dimroth et al.'s $E_{\text{T}(30)}$ polarity scale value,^{41,44} which was derived from the spectral behavior of 2,6-diphenyl-4-(2,4,6-triphenylpyridinio)phenoxide. Thus, the maxima absorption band energy ($E_{\text{abs PRODAN}}$) and the maxima emission band energy ($E_{\text{em PRODAN}}$) for the different solvents shown in Table 1 were correlated with the $E_{\text{T}(30)}$ polarity scale.^{41,44} Equations 6 and 7 show the linear relationships that these parameters experience with the $E_{\text{T}(30)}$ value.

$$E_{\text{T}(30)} = 345 \pm 5 - (3.78 \pm 0.02)E_{\text{abs PRODAN}} \quad (6)$$

$$n = 26, r = 0.95$$

$$E_{\text{T}(30)} = 147 \pm 5 - (1.62 \pm 0.02)E_{\text{em PRODAN}} \quad (7)$$

$$n = 23, r = 0.98$$

In a previous work,⁴⁵ it was demonstrated that the transition energy of the visible absorption band of 1-methyl-8-oxyquinolinium betaine (QB), although it is sensitive to the same solvent parameters as PRODAN, π^* and the specific interaction parameter α , could be used to monitor successfully the polarity of the microenvironment of AOT reverse micelles.⁴⁶ Clearly, as QB, PRODAN is eminently suitable as a probe for micropolarity which will help us to monitor the microenvironment of the LUV DOPC bilayer.

Behavior of PRODAN in Water. Parts A and B of Figure 2 show the dependence of the PRODAN absorption and emission bands in water, respectively, as a function of the PRODAN concentration. The results show a sharp decrease of the molar extinction coefficient (ϵ) (Figure 2A) and that a new emission band emerges near 430 nm (Figure 2B) upon increasing concentration. Also, the Lambert–Beer law is not obeyed in the whole concentration range studied (Figure 2A). The photophysical behavior of PRODAN in water, although other authors have investigated it, is not yet completely understood.

TABLE 2: Fluorescence Lifetimes (τ , ns)^a of PRODAN in Water and in LUVs of DOPC ([PRODAN] = 3×10^{-5} M)

[DOPC] (mg/mL)	λ_{exc} : 360 nm λ_{em} : 435 nm	λ_{exc} : 360 nm λ_{em} : 525 nm
0		$\tau_1 = 2.27 \pm 0.01$ (43.5%) ^b $\tau_2 = 0.65 \pm 0.03$ (56.5%) ^b $\chi^2 = 1.16$ $\langle r_m \rangle = 0.018 \pm 0.005^c$
	$\tau_1 = 2.69 \pm 0.09$ (44.6%) $\tau_2 = 0.30 \pm 0.04$ (30.2%) $\tau_3 = 14.60 \pm 0.03$ (25.2%) $\chi^2 = 1.11$ $\langle r_{\text{ag}} \rangle = 0.045 \pm 0.005^c$	$\tau_1 = 2.58 \pm 0.06$ (36.15%) $\tau_2 = 0.81 \pm 0.03$ (63.85%) $\chi^2 = 1.39$
0.05	$\tau_1 = 3.01 \pm 0.01$ (16%) $\tau_2 = 0.26 \pm 0.02$ (34%) $\tau_3 = 1.15 \pm 0.09$ (49%) $\chi^2 = 1.2$	$\tau_1 = 3.19 \pm 0.01$ (22%) $\tau_2 = 0.80 \pm 0.03$ (78%) $\chi^2 = 1.29$
0.1	$\tau_1 = 3.26 \pm 0.09$ (14%) $\tau_2 = 0.21 \pm 0.05$ (47%) $\tau_3 = 1.40 \pm 0.04$ (38%) $\chi^2 = 1.11$	$\tau_1 = 4.17 \pm 0.06$ (73%) $\tau_2 = 1.52 \pm 0.03$ (27%) $\chi^2 = 0.9$
0.25	$\tau_1 = 4.66 \pm 0.09$ (55%) $\tau_2 = 0.17 \pm 0.05$ (5%) $\tau_3 = 1.19 \pm 0.07$ (40%) $\chi^2 = 1.3$	$\tau = 3.88 \pm 0.06$ $\chi^2 = 0.9$
1	$\tau_1 = 3.35 \pm 0.09$ (52%) $\tau_2 = 1.26 \pm 0.04$ (48%) $\chi^2 = 1.2$	$\tau = 4.11 \pm 0.09$ $\chi^2 = 1.7$
5	$\tau_1 = 3.33 \pm 0.09$ (40%) $\tau_2 = 1.26 \pm 0.04$ (60%) $\chi^2 = 1.19$	$\tau = 4.08 \pm 0.09$ $\chi^2 = 1.79$

^a The values in parentheses are the contribution of the species obtained from the fit. ^b [PRODAN] = 1×10^{-6} M. ^c $\langle r_m \rangle$ and $\langle r_{\text{ag}} \rangle$ are the steady-state anisotropy for the monomer and the aggregate, respectively.

The extra blue-edge emission band at $\lambda = 430$ nm, which is excitation wavelength and PRODAN concentration dependent, has been interpreted in different ways: (i) due to solute–solvent complexes formed via hydrogen bonding interaction,^{20,47} (ii) due to trace water-soluble impurities in the sample,³³ and (iii) due to the molecule association to form n -mers (largely unsolvated) which can grow to eventually produce microcrystals.^{31,32} The results presented in Figure 2A and B seem to indicate that PRODAN molecules aggregate in water upon increasing concentration. The emission results (Figure 2B) show that at low probe concentration only one band at ~ 520 nm is present and is assigned to the monomeric species, while at higher concentration the new band peaked at 430 nm is assigned to the aggregate. The ratio of the emission spectrum measured at $\lambda = 430$ nm and $\lambda = 523$ nm (I^{430}/I^{523}) is shown as a function of PRODAN concentration in Figure 3. There is a break at [PRODAN] $\sim 1 \times 10^{-5}$ M, which can be thought as the threshold concentration where the dye starts to aggregate. The absence of a clear isosbestic point in the absorption spectrum of PRODAN in water suggests that the aggregation process may include higher order aggregates than simple monomer–dimer equilibrium but is a matter of further investigation the exact nature of this aggregate.

The “aggregation process” was also explored using single photon counting and steady-state anisotropy techniques. Table 2 shows the fluorescence lifetimes of the molecular probe at different dye concentrations and emission wavelengths. The table shows that, at [PRODAN] = 1×10^{-6} M when the probe exists only as a monomer, the emission decay fits well to a biexponential function which is in agreement with the results obtained by other authors for PRODAN in water.³¹ The biexponential decay obtained for PRODAN is not surprising, since it is known^{18,48,49} that the absorption band of PRODAN

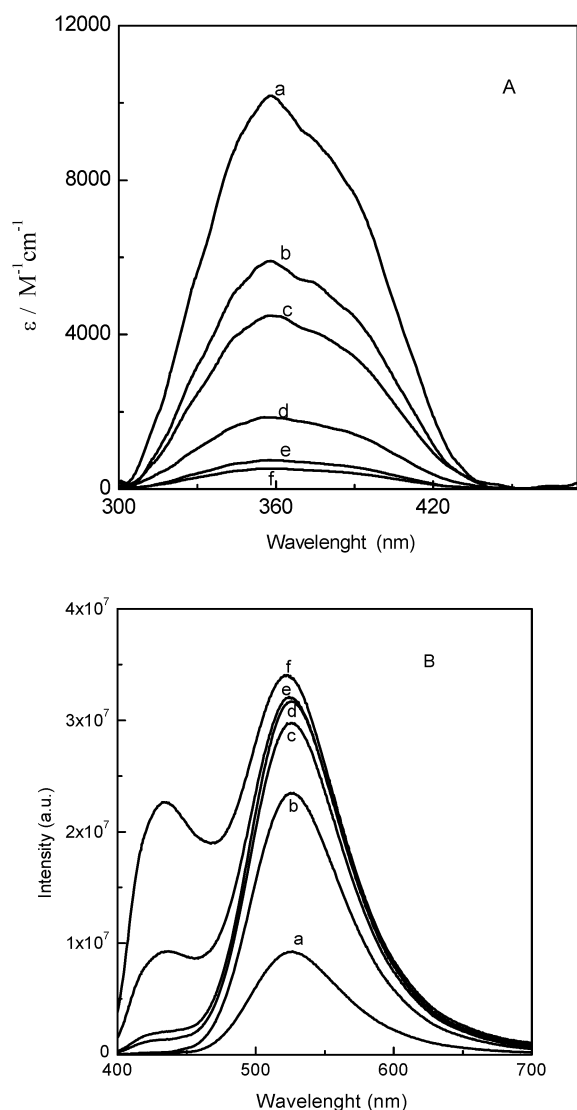


Figure 2. (A) Molar extinction coefficient (ϵ) of PRODAN in water as a function of PRODAN concentration. [PRODAN] (M) = (a) 2.7×10^{-6} , (b) 5.3×10^{-6} , (c) 8.0×10^{-6} , (d) 1.7×10^{-5} , (e) 2.2×10^{-5} , and (f) 3.5×10^{-5} . (B) Emission spectra (λ_{exc} : 389 nm) of PRODAN in water as a function of PRODAN concentration. [PRODAN] (M) = (a) 2.7×10^{-6} , (b) 5.3×10^{-6} , (c) 8.0×10^{-6} , (d) 1.7×10^{-5} , (e) 2.2×10^{-5} , and (f) 3.5×10^{-5} .

corresponds to a superposition of two $\pi \rightarrow \pi^*$ transitions mainly localized on the naphthalene ring with a rather small charge transfer from the dimethylamino group to the carbonyl group. At [PRODAN] = 3×10^{-5} M and λ_{em} = 435 nm, the decay fits nice to a triexponential function with a new component of 14.6 ns. This fluorescence lifetime is not observed at λ_{em} = 525 nm where only the monomer is detected. Thus, we assign the 14.6 ns component to the PRODAN aggregate species. Other authors^{20,31–33} have attempted to characterize the aggregates using the same techniques, but the results found besides not being fully explained are quite different from the ones obtained in our laboratory. For example, Flora et al.³² found a value of the fluorescence lifetime of 2.07 ns for the PRODAN aggregates and a value of 1.45 ns for the monomer. In addition, they found that the anisotropy for the aggregate is significantly higher at shorter wavelengths than at longer wavelengths with respect to the monomer. Using the lifetime values shown above, they calculated the volume of the respective rotating units (V_{430} and V_{595} , respectively) in water solution using the Perrin equation

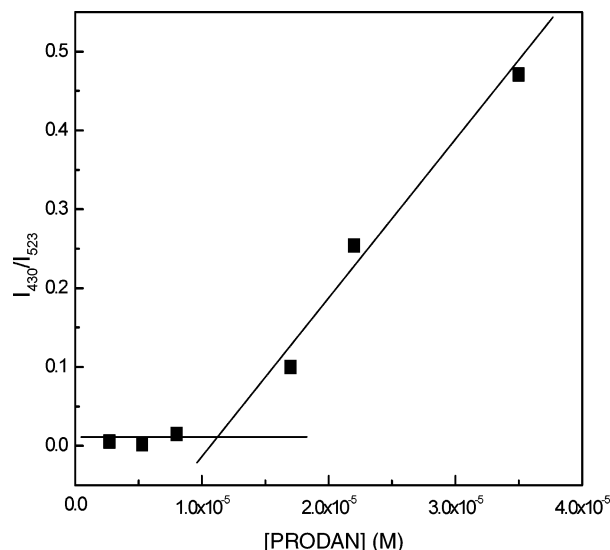


Figure 3. Intensity ratio of 430 nm to 523 nm fluorescence bands of PRODAN in water. λ_{exc} : 389 nm.

(eq 2). The volumes found for the rotating units were V_{430} = 730 mL mol⁻¹ for the aggregate and V_{595} = 284 mL mol⁻¹ for the monomer. On the other hand, from single photon counting measurements, Balter et al.²⁰ found that the fluorescence decay for PRODAN in water fits well to a double exponential with lifetime values of $\tau_1 \sim 0.5$ ns and $\tau_2 \sim 1.9$ ns. If the emission decay is monitored around the blue edge of the emission spectra, a small contribution of a long-lived component (~ 13 ns) appears. However, the origin of this component was not clarified. Sun et al.³¹ suggested that this long-lived component is probably due to the PRODAN aggregate species.

Taking into account our fluorescence lifetime values gathered in Table 2 and our assignment, it is clear that the aggregate's lifetime used before³² to calculate V_{430} is not correct. For this reason, we recalculated the volumes using the steady-state anisotropy data shown in Table 2 and eq 2. With our experimentally determined lifetimes in water, the following rotational correlation times are obtained: ϕ_{430} = 2.26 ns and ϕ_{525} = 0.09 ns. From these values, the corresponding volumes of the rotating unit at 25 °C are V_{430} = 5590 mL mol⁻¹ and V_{525} = 222 mL mol⁻¹. The volume for the monomer is quite similar to the one obtained by Flora et al.,³² but the one for the aggregate is very different. We want to stress that, given that the volumes of the aggregate and the monomer have been calculated from eq 2, which is deduced from the simplest sphere model without any modification,¹⁴ it is not possible, from these values, to deduce quantitatively the amount of PRODAN molecules that are involved in the aggregate. It seems to us that several dye monomers are involved in PRODAN's aggregate. To quantify the number of monomers forming the aggregate from the anisotropy data, it will be necessary to deduce a more complete equation that includes the dye molecular shape (prolate or oblate) and stick and slip boundary conditions. This is out of the scope of this work.

Study in DOPC LUVs. To the best of our knowledge, the location of PRODAN in LUVs of the DOPC system and the influence that this media has on the aggregation process of the probe has not been previously explored. Thus, it seems to us that it is relevant and interesting to investigate what is the effect that the DOPC bilayer has on the PRODAN characteristics.

First, the behavior of PRODAN monomer has been studied by varying the phospholipid concentration at [PRODAN] = 5×10^{-6} M. Figure 4 shows the emission spectra at different

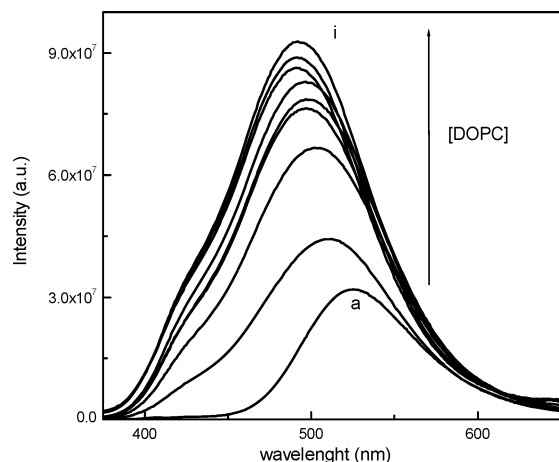


Figure 4. Emission spectra (λ_{exc} : 319 nm) of PRODAN in LUVs of DOPC as a function of DOPC concentration. [DOPC] (mg/mL) = (a) 0.00, (b) 0.05, (c) 0.10, (d) 0.15, (e) 0.20, (f) 0.40, (g) 1.25, (h) 2.00, and (i) 2.63. [PRODAN] = 5×10^{-6} M.

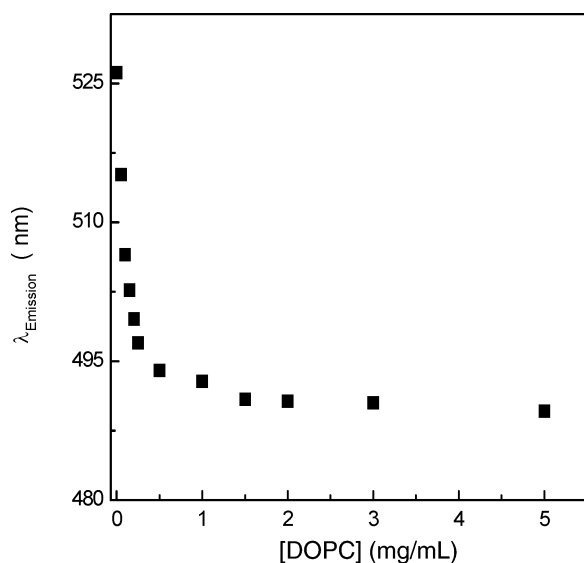


Figure 5. Variation of PRODAN emission maxima as a function of DOPC concentration. λ_{exc} : 319 nm. [PRODAN] = 5×10^{-6} M.

[DOPC] values. As the phospholipid concentration increases, there is a hypsochromic shift of the emission and absorption band (results not shown). Considering the results shown previously in the homogeneous section (eqs 4 and 5), this hypsochromic shift is probably due to the incorporation of PRODAN into a less polar environment, compared with water, that is, the bilayer of the vesicles. In other words, PRODAN, being more soluble in a nonpolar environment, experiments a partition into the LUV bilayer. Similar results have been shown for PRODAN in another phospholipid's vesicles.^{9,12,19,28–30} Figure 5, which shows the shift of the emission band as a function of the phospholipid concentration, clearly demonstrates the incorporation of the probe into the bilayer. Moreover, the result shows that at [DOPC] \sim 1 mg/mL there is no more shift of the emission band which is suggesting that PRODAN exists exclusively in the bilayer. Figure 6 shows the steady-state anisotropy $\langle r \rangle$ of PRODAN varying the DOPC concentration. The data show the change in the fluidity of the microenvironment that PRODAN senses upon the incorporation into the bilayer. At [DOPC] < 1 mg/mL, where PRODAN exists mostly in the water pseudophase, that microenvironment is quite fluid. On the contrary, as the phospholipid concentration increases, a

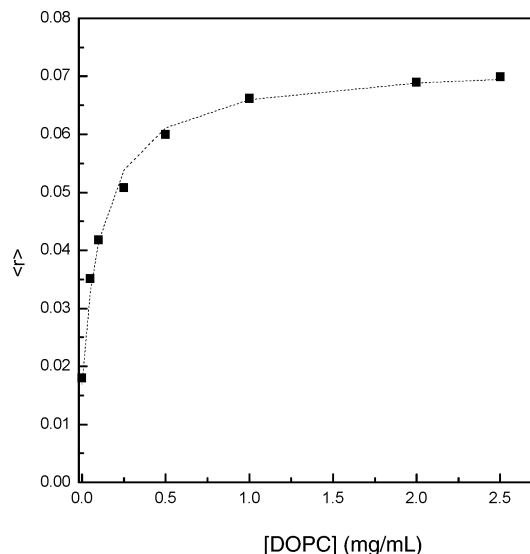


Figure 6. Steady-state anisotropy $\langle r \rangle$ for PRODAN in LUVs of DOPC varying [DOPC]. λ_{exc} : 319 nm. λ_{em} : 490 nm. [PRODAN] = 1×10^{-6} M. The dotted line values were fitted with eq 12.

more rigid medium is sensed, reflecting the incorporation of the probe into the bilayer. At [DOPC] > 1 mg/mL, the anisotropy value reaches a plateau which probably indicates that PRODAN exists predominantly in the viscous DOPC bilayer.³⁰ From the changes in the steady-state anisotropy $\langle r \rangle$ values with the phospholipid concentration (Figure 6), we calculate the value of the partition constant (K_p) that PRODAN undergoes in this system.⁵⁰ The PRODAN partition process between the DOPC vesicles and water is treated within the framework of the pseudophase model.^{50–55} In this model, only two solubilization sites are considered, that is, the water and the vesicle interface (i.e., all of the DOPC molecules). Thus, the distribution of PRODAN between the bilayer and the water pseudophase defined in eq 8 is expressed in terms of the partition constant (K_p) shown in eq 9:



$$K_p = \frac{[\text{PRODAN}]_b^{\#}}{[\text{PRODAN}]_w} \quad (9)$$

The terms in brackets represent PRODAN in water (w) and bound (b) to the bilayer in terms of local concentrations. If [PRODAN]_b is the analytical (bulk) concentration of vesicle bound substrate, eq 10 holds.

$$[\text{PRODAN}]_b^{\#} = \frac{[\text{PRODAN}]_b}{[\text{DOPC}]} \quad (10)$$

and hence K_p can be expressed as in eq 11

$$K_p = \frac{[\text{PRODAN}]_b}{[\text{PRODAN}]_w [\text{DOPC}]} \quad (11)$$

where [PRODAN]_b is the analytical concentration of the substrate incorporated into the bilayer, [PRODAN]_w is the concentration of the substrate in the water bulk, and [DOPC] is the phospholipid concentration. This equation applies when [PRODAN]_T \ll [DOPC].

Equation 12 is deduced from the additivity law for anisotropy^{14,50} and shows the dependence between $\langle r \rangle$ and the

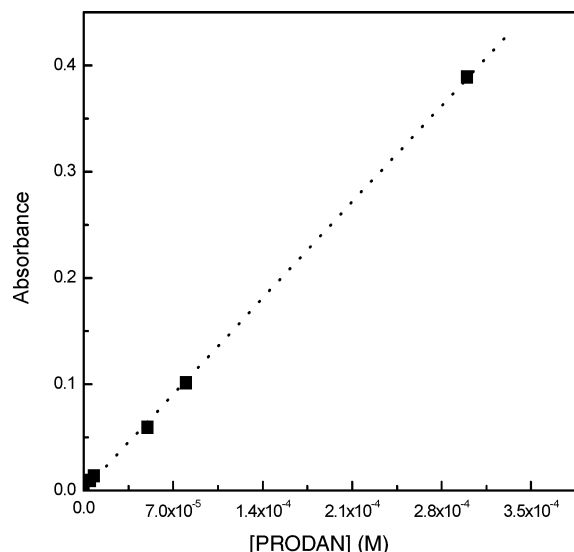


Figure 7. Lambert–Beer law of $\lambda_{\text{abs}} = 356$ nm of PRODAN in LUVs of DOPC. [DOPC] = 1 mg/mL.

DOPC concentration.

$$\langle r \rangle = \frac{\langle r_w \rangle + \langle r_b \rangle K_p [\text{DOPC}]}{(1 + K_p [\text{DOPC}])} \quad (12)$$

where $\langle r \rangle$ is the anisotropy of the mixture, $\langle r_w \rangle$ and $\langle r_b \rangle$ are the anisotropies of the water and bound PRODAN species, respectively, and [DOPC] is the phospholipid concentration. Thus, using a least-squares fit of eq 12, we calculate the value of K_p for PRODAN and find a value of $16.4 \pm 2 \text{ g/mL}^{-1}$ or $12\,900 \pm 1300 \text{ M}^{-1}$ considering that the molecular weight of DOPC is 786.15 g/mol . Figure 6 shows, with the dotted line, how the data can be fitted with eq 12. The value of K_p shows that, at [DOPC] = 1 mg/mL, 94% of the total PRODAN concentration exists exclusively in the DOPC bilayer (eq 11) and the amount that can partition to the water is very small and cannot be detected experimentally even at the highest PRODAN concentration studied, that is, $3 \times 10^{-4} \text{ M}$. The result demonstrates that PRODAN is a powerful probe for monitoring bilayer properties because it resides exclusively in this pseudophase. Other authors^{19,24} have also suggested that there is a partition of PRODAN between the bilayer and water for multilamellar vesicles made of dilauroyl and dipalmitoyl phosphatidylcholine (DLPC and DPPC, respectively), being more favorable in the liquid-crystalline phase. However, the results presented here for LUVs of DOPC do not show any evidence of the presence of PRODAN in water when [DOPC] > 1 mg/mL (Figure 7 and Table 2). Also, in the emission spectra, the band which corresponds to the aggregate in water is absent in the whole PRODAN concentration studied (results not shown).

To investigate if the aggregation process occurs in the vesicles, the absorption spectra were recorded at different PRODAN concentrations at [DOPC] = 1 mg/mL. Figure 7 shows that, under these experimental conditions, the system obeys the Lambert–Beer law in the whole [PRODAN] range studied, namely, 5×10^{-6} – $3 \times 10^{-4} \text{ M}$. The results reveal that the PRODAN does not aggregate in the vesicle bilayer, due to the expected higher solubility of the probe in the nonpolar environment in comparison with water.

Red-Edge Excitation Shift Studies (REES). The steady-state and time-resolved results we report prompted us to explore the behavior of the probe with a red-edge excitation shift (REES) investigation.¹⁴ When solvent relaxation occurs on a time scale

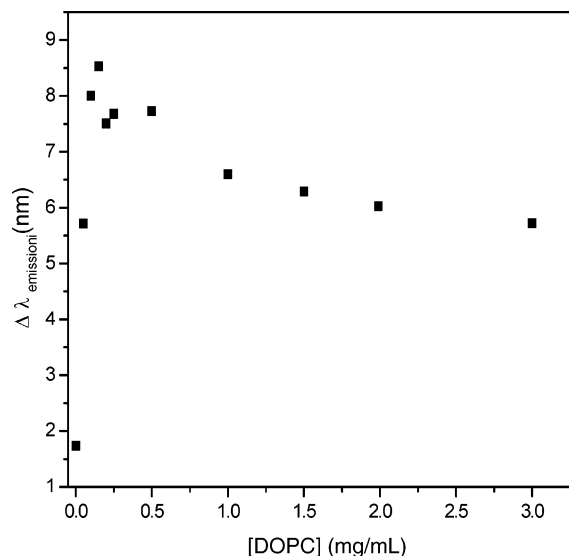


Figure 8. $\Delta\lambda_{\text{em}} = (\lambda_{\text{em(exc 410nm)}} - \lambda_{\text{em(exc 319nm)}})$ for PRODAN in LUVs of DOPC as a function of DOPC concentration. [PRODAN] = $5 \times 10^{-6} \text{ M}$.

comparable to or longer than the fluorescence lifetime, then the slow excited-state relaxation leads the peak of the emission spectrum to shift to longer wavelength as the excitation wavelength shifts to longer wavelength. The REES reflects slow solvent motion or motional restriction of the chromophores.^{14,16,17}

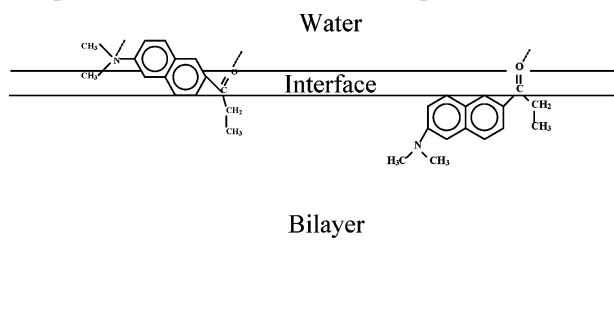
For PRODAN, the REES is characterized by the difference in the emission peak when exciting at 410 and 319 nm

$$\Delta\lambda_{\text{emission}} = \lambda_{\text{em}}(\text{excitation} = 410 \text{ nm}) - \lambda_{\text{em}}(\text{excitation} = 319 \text{ nm}) \quad (13)$$

Figure 8 shows that the emission spectra in the vesicles not only depend on the excitation wavelength in the red edge of the PRODAN absorption spectra but also depend on the DOPC concentration. A couple of factors can explain the observed changes as follows: (i) the incorporation of the molecular probe from the water into the bilayer giving more than one emitting species and/or (ii) PRODAN exists in a dipolar relaxing environment (i.e., the dipolar relaxation time for the solvent shell must be comparable to or longer than the fluorescence lifetime of the probe), so the fluorescence occurs from various partially relaxed states, phenomena that are observed in very viscous solutions or condensed phases.¹ It is worthy to mention that Hutterer et al.⁵⁶ using the solvent relaxation technique demonstrated the slow solvent relaxation kinetics of PRODAN, located closer to the lipid/water interface of small unilamellar vesicles composed of different mixtures of phosphatidyl-L-serine and phosphatidylcholine.

Regarding the effect of the phospholipid concentration on the REES, Figure 8 shows that at low [DOPC] (<0.15 mg/mL) there is probe in the water and the bilayer.²⁴ The K_p value shows that, at [DOPC] = 0.15 mg/mL, 30% of the total PRODAN concentration is still in the water bulk pseudophase. PRODAN inside the aggregate is located in a motionally restricted medium compared with the molecules in water. Hence, there is a composite of effects i and ii mentioned above, with the partitioning to water being the predominant effect. At higher DOPC concentration, effect ii starts to be the dominant factor, and once PRODAN exists entirely in the bilayer at [DOPC] = 1 mg/mL, effect i is no longer present. Surprisingly, the REES still decreases above this DOPC concentration although in less magnitude. Chong³⁰ has investigated the effects of the hydro-

SCHEME 1: Representation of PRODAN at the Polar (toward the Water) and Less Polar (toward the Lipid Tails) Environments for the Probe Completely Incorporated into the Membrane (Adapted from ref 30)



static pressure on the location of PRODAN in the lipid bilayers made of dimyristoyl-L- α -phosphatidylcholine (DMPC) multilamellar vesicles and egg yolk phosphatidylcholines. He found changes in the emission spectra which were attributed to a pressure-induced relocation of the molecules residing at the water/lipid interface, the polar microenvironment (peaks at 510 nm) to a less polar environment which is not the hydrocarbon core and peaks at 435 nm, with an isoemissive point in the egg yolk phosphatidylcholine system. The disposition of the two emitting species is shown in Scheme 1. Krasnowska et al.²⁴ have suggested that the proposed attribution of PRODAN emission from the probe location at various depths along the bilayer is unlikely because of the partition of the probe to the water. However, they used a low phospholipid concentration (around 0.12 mg/mL) where we have shown before part of the probe is still in the water (Figures 4 and 8).

Consequently, the results observed above [DOPC] = 1 mg/mL in Figure 8 (where the entire probe exists incorporated into the bilayer) can be explained considering the model proposed by Chong³⁰ (see Scheme 1). PRODAN in the bilayer exists part in the polar environment (the viscous interfacial region with peaks around 490 nm) and part in the less polar one with a less viscous microenvironment corresponding to the band at ~426 nm. Hence, the probe located deep inside the bilayer is surrounded by a less motionally restricted microenvironment and the dependence of the emission band with the excitation wavelength is less notorious. Moreover, the appearance of a shoulder at ~426 nm as the phospholipid concentration increases shown in Figure 4 could be indicating the appearance of the emitting PRODAN species located in the less polar environment. The lack of an isoemissive point in Figure 4 is probably due to the scattering of the solution that cannot be completely subtracted despite the use of blank vesicle solutions. Nonetheless, the decrease in the value of REES above [DOPC] = 1 mg/mL can also indicate a change in the media relaxation around the probe in the bilayer.⁵⁶ However, the measurements of the fluorescence lifetimes (Table 2) support the previous conclusions. At [DOPC] < 0.1 mg/mL, two emitting species exist: one in water with an emission decay that fits well to a biexponential function and the other in the bilayer ($\tau_3 = 1.15$ ns). Once the probe exists inside the bilayer ([DOPC] > 1 mg/mL), the emission decay, at $\lambda_{em} = 525$ nm, fits well to a monoexponential function and gives a fluorescence lifetime which corresponds to the species emitting from the polar environment (Scheme 1). At $\lambda_{em} = 435$ nm, the emission decay fits adequately to a biexponential function with fluorescence lifetimes matching to the species in the polar environment and in the nonpolar one. Also, the contribution of these species increases with the DOPC concentration in agreement with the

result shown in Figure 8. At [DOPC] = 0.25 mg/mL, the contribution of PRODAN from water is almost nill, as expected. Moreover, contrary to the results found in water, there is no evidence of aggregates at any DOPC concentration.

Micropolarity. As was shown in eq 7, E_{em} PRODAN could be used to determine the micropolarity of the DOPC LUV bilayer through the well-known solvent parameter $E_{T(30)}$.⁴¹ We chose [DOPC] = 1 mg/mL because PRODAN exists exclusively in the bilayer. For $\lambda_{em}^{max} = 490$ nm which is the band that corresponds to the probe in the polar part of the bilayer (Scheme 1), a value of $E_{T(30)} = 53.8$ kcal/mol is found. This value is similar to the $E_{T(30)}$ value in methanol⁴⁴ and corresponds to the micropolarity of the polar part of the bilayer. For $\lambda_{em}^{shoulder} = 423$ nm, which is the band that corresponds to PRODAN in the less polar part of the bilayer, a value of $E_{T(30)} = 36.98$ kcal/mol is found which is similar to the $E_{T(30)}$ values in solvents such as tetrahydrofuran and anisole. This value corresponds to the micropolarity of the less polar part of the bilayer where PRODAN exists. Furthermore, the $E_{T(30)}$ values that PRODAN senses inside the vesicles are quite different from the polarity of water ($E_{T(30)} = 63.1$ kcal/mol).⁴⁴ Indeed, the micropolarity that the ground state of PRODAN senses (eq 6) at [DOPC] = 1 mg/mL gives a value of $E_{T(30)} = 36$ kcal/mol, which is in agreement with the one obtained by the probe located in the less polar environment of the bilayer.

Conclusions

The results show that, in homogeneous media, the PRODAN absorption band is sensitive to the polarity–polarizability (π^*) and the hydrogen bond donor ability (α) parameters of the environment. PRODAN in the excited state is even more sensitive to these parameters and to the hydrogen bond acceptor ability (β) of the media. Its transition energy (expressed in kcal/mol) for both absorption and emission bands gives a linear correlation with the well-known polarity parameter $E_{T(30)}$. From the absorption and emission bands, also it is demonstrated that PRODAN forms aggregates in water. The monomer has two fluorescence lifetimes, 2.27 and 0.65 ns, while the aggregate has a lifetime of 14.6 ns. Using steady-state anisotropy measurements, the calculated volumes of the aggregate and the monomer are 5590 and 222 mL mol⁻¹, respectively. This indicates that the aggregate may have several monomer molecules.

PRODAN is fully characterized in LUV vesicles of DOPC. It is shown that, at [DOPC] > 1 mg/mL, it exists completely incorporated in its monomer form and senses two different microenvironments within the bilayer, a polar region in the interface near the water and a less polar region and also less viscous environment between the phospholipid tails. These environments were characterized by their fluorescence lifetimes (τ), showing that PRODAN has a higher τ value in the polar region than in the less polar region. Moreover, PRODAN also senses the micropolarity of these two different regions of the bilayer which are comparable to methanol and tetrahydrofuran.

In summary, this work gives novel and relevant results for the quantitative description of the aggregation process that PRODAN undergoes in water as well as the partition process that the molecule undergoes in the DOPC LUV systems. Moreover, the results reveal some aspects yet unexplored about the DOPC vesicle bilayers like the capacity that the membrane has to host molecular probes as monomers, important results in the field of the nonlinear optics, for example, in the preparation of dye lasers which require a noninteracting monomer form of the dye. Also, the data reveal the micro-

polarity value of two different zones in the bilayer, results very powerful especially to take advantage of this “green” system as nanoreactors.

Acknowledgment. Financial support from the Consejo Nacional de Investigaciones Científicas y Técnicas (CONICET), Universidad Nacional de Río Cuarto, Fundación Antorchas and Agencia Nacional de Promoción Científica y Técnica is gratefully acknowledged. J.J.S., M.A.B., and N.M.C. hold a research position at CONICET. F.M. thanks CONICET for a research fellowship.

References and Notes

- (1) Chattopadhyay, A.; Mukherjee, S. *Biochemistry* **1993**, *32*, 3804.
- (2) Parasassi, T.; De Stasio, G.; d'Ubaldo A.; Gratton, E. *Biophys. J.* **1990**, *57*, 1179.
- (3) Teissie, J.; Tsong, T. Y. *Biochemistry* **1981**, *20*, 1548.
- (4) Correa, N. M.; Schelly, Z. A. *Langmuir* **1998**, *14*, 5802.
- (5) Correa, N. M.; Schelly, Z. A. *J. Phys. Chem. B* **1998**, *102*, 9319.
- (6) Ashgarian, N.; Schelly, Z. A. *Biochim. Biophys. Acta* **1999**, *1418*, 295.
- (7) Correa, N. M.; Schelly, Z. A. Zhang, H. J. *Am. Chem. Soc.* **2000**, *122*, 6432.
- (8) Rex, S. *Biophys. Chem.* **1996**, *58*, 75.
- (9) Chong, P. L. G.; Capes, S.; Wong, P. T. T. *Biochemistry* **1989**, *28*, 8358.
- (10) Seelig, J.; McDonald, P. M.; Scherer, P. G. *Biochemistry* **1987**, *26*, 7535.
- (11) Devaux, P. H.; Signeuret, M. *Biochim. Biophys. Acta* **1985**, *822*, 63.
- (12) Parasassi, T.; De Stasio, G.; Ravagnan, G.; Rusch, R. M.; Gratton, E. *Biophys. J.* **1991**, *60*, 179.
- (13) Ramani, K.; Balasubramanian, S. V. *Biochim. Biophys. Acta* **2003**, *1618*, 67.
- (14) Lakowicz, J. R. *Principles of Fluorescence Spectroscopy*, 2nd ed.; Kluwer Academic: New York, 1999.
- (15) Demchenko, A. P. *Luminescence* **2002**, *11*, 19.
- (16) Milhaud, J. *Biochim. Biophys. Acta* **2004**, *1663*, 19.
- (17) Chattopadhyay, A. *Chem. Phys. Lipids* **2003**, *122*, 3.
- (18) Weber, G.; Farris, F. J. *Biochemistry* **1979**, *18*, 3075.
- (19) Krasnowska, E. K.; Bagatolli, L. A.; Gratton, E.; Parasassi, T. *Biochim. Biophys. Acta* **2001**, *1511*, 330.
- (20) Balter, A.; Nowak, W.; Pawelkiewicz, W.; Kowalczyk, A. *Chem. Phys. Lett.* **1988**, *143*, 565.
- (21) Catalan, J.; Perez, P.; Laynez, J.; Blanco, F. G. *J. Fluoresc.* **1991**, *1*, 215.
- (22) Zurawsky, W. P.; Scarlata, S. F. *J. Phys. Chem.* **1992**, *96*, 6012.
- (23) Moreno, F.; Corrales, S.; Sevilla, P.; Blanco, F. G.; Diaz, C.; Catalán, J. *Helv. Chim. Acta* **2001**, *84*, 3306.
- (24) Krasnowska, E. K.; Gratton, E.; Parasassi, T. *Biophys. J.* **1998**, *74*, 1984.
- (25) Parasassi, T.; Krasnowska, E. K.; Bagatolli, L. A.; Gratton, E. *J. Fluoresc.* **1998**, *8*, 365.
- (26) Hutterer, R.; Schneider, F. W.; Sprinz, H.; Hof, M. *Biophys. Chem.* **1996**, *151*.
- (27) Hutterer, R.; Parusel, A. B. J.; Hof, M. *J. Fluoresc.* **1998**, *8*, 389.
- (28) Zeng, J. W.; Chong, P. L. *Biochemistry* **1991**, *30*, 9485.
- (29) Rottenberg, H. *Biochemistry* **1992**, *31*, 9473.
- (30) Chong, P. L. G. *Biochemistry* **1988**, *27*, 399.
- (31) Sun, S.; Heitz, M. P.; Perez, S. A.; Colón, L. A.; Bruckenstein, S.; Bright, F. *Appl. Spectrosc.* **1997**, *51*, 1316.
- (32) Flora, K. K.; Brennan, J. D. *J. Phys. Chem. B* **2001**, *105*, 12003.
- (33) Bunker, C. E.; Bowen, T. L.; Sun, Y.-P. *Photochem. Photobiol.* **1993**, *4*, 499.
- (34) Lewis, R. N. A. H.; McElhaney, R. N. In *The Structure of Biological Membranes*; Yeagle, P., Ed.; CRC Press: Boca Raton, FL, 1992; p 92.
- (35) Mayer, L. D.; Hope, M. J.; Cullis, P. R. *Biochim. Biophys. Acta* **1986**, *858*, 161.
- (36) Ashgarian, N.; Wu, X.; Meline, R. L.; Derecskei, B.; Cheng, H.; Schelly, Z. A. *J. Mol. Liq.* **1997**, *72*, 315.
- (37) Hope, M. J.; Bally, M. B.; Webb, G.; Cullis, P. R. *Biochim. Biophys. Acta* **1985**, *812*, 55.
- (38) Narang, U.; Jordan, J. D.; Bright, F. V.; Prasad, P. N. *J. Phys. Chem.* **1994**, *98*, 8101.
- (39) O'Connor, D. V.; Phillips, D. *Time-Correlated Single Photon Counting*; Academic Press: New York, 1983; Chapter 6.
- (40) Kamlet, M. J.; Abboud, J. L. M.; Abraham, M. H.; Taft, R. W. J. *J. Org. Chem.* **1983**, *48*, 2877.
- (41) Marcus, Y. *Chem. Soc. Rev.* **1993**, 409.
- (42) Abboud, J. L. M.; Notario, R. *Pure Appl. Chem.* **1999**, *71*, 645.
- (43) Laurence, C.; Nicolet, P.; Dalati, M. T.; Abboud, J. L. M.; Notario, R. *J. Phys. Chem.* **1994**, *98*, 5807.
- (44) Reichardt, C. In *Solvents and Solvent Effects in Organic Chemistry*, 2nd ed.; VCH: Germany, 1990.
- (45) Ueda, M.; Schelly, Z. A. *Langmuir* **1989**, *5*, 1005.
- (46) Correa, N. M.; Biasutti, M. A.; Silber, J. J. *J. Colloid Interface Sci.* **1995**, *172*, 71.
- (47) Karukstis, K. K.; Frazier, A. A.; Martula, D. S.; Whiles, J. A. *J. Phys. Chem.* **1996**, *100*, 11133.
- (48) Nowak, W.; Adamczak, P.; Balter, A. *THEOCHEM* **1986**, *139*, 13.
- (49) Parusel, A. B. J.; Nowak, W.; Grimme, S.; Köhler, G. *J. Phys. Chem. A* **1998**, *102*, 7149.
- (50) Falcone, R. D.; Correa, N. M.; Biasutti, M. A.; Silber, J. J. *J. Colloid Interface Sci.* **2006**, *296*, 356.
- (51) Lissi, E. A.; Abuin, E. A.; Rubio, M. A.; Cerón, A. *Langmuir* **2000**, *16*, 178.
- (52) Abuin, E.; Lissi, E.; Duarte, R.; Silber, J. J.; Biasutti, M. A. *Langmuir* **2002**, *18*, 8340.
- (53) Silber, J. J.; Biasutti, M. A.; Abuin, E.; Lissi, E. *Adv. Colloid Interface Sci.* **1999**, *82*, 189.
- (54) Encinas, M. V.; Lissi, E. *Chem. Phys. Lett.* **1986**, *132*, 545.
- (55) Aguilar, L. F.; Abuin, E.; Lissi, E. *Arch. Biochem. Biophys.* **2001**, *388*, 231.
- (56) Hutterer, R.; Schneider, F. W.; Hermens, W. Th.; Wagenvoord, R.; Hof, M. *Biochim. Biophys. Acta Biomembr.* **1998**, *1414*, 155.